

COMPARING KINETIC AND HYDRODYNAMICAL MODELS FOR ELECTRON TRANSPORT IN MONOLAYER GRAPHENE

MARCO COCO*, ARMANDO MAJORANA†, GIOVANNI MASCALI‡,
VITTORIO ROMANO†

* Department of Mathematics and Computer Science
University of Catania
Viale A. Doria 6, 95125 Catania, Italy
e-mail: mcoco@dmi.unict.it

† Department of Industrial Engineering
University of Catania
Viale A. Doria 6, 95125 Catania, Italy
e-mail: majorana@dii.unict.it, romano@dii.unict.it

‡ Department of Mathematics and Computer Science
University of Calabria
and INFN-Gruppo c. 87036 Cosenza, Rende, Italy
e-mail: giovanni.mascali@unical.it

Key words: Graphene, Boltzmann Transport Equation, Discontinuous Galerkin Method, Hydrodynamical Models for Semiconductors.

Abstract. The aim of this work is to compare, in monolayer graphene, solutions of the electron Boltzmann equation, obtained with a discontinuous Galerkin method, with those of a hydrodynamical model based on the Maximum Entropy Principle.

1 INTRODUCTION

Graphene is a gapless semiconductor made of a single layer of carbon atoms arranged into a honeycomb hexagonal lattice [1]. In view of applications in graphene-based electron devices, it is crucial to understand the basic transport properties of this material.

A physically accurate model is given by a semiclassical transport equation whose scattering terms have been deeply analyzed recently [2, 3, 4]. Due to the computational difficulties, the most part of the available solutions have been obtained by direct Monte Carlo simulations. A different approach has been employed in [5].

For computer aided design (CAD) purposes, it could be useful to have macroscopic

models like drift-diffusion, energy-transport and hydrodynamical ones. Macroscopic models have been proposed, for example, in [6, 7, 8].

The aim of this work is to assess the validity of the hydrodynamical model based on the Maximum Entropy Principle (MEP) [7], by comparing the solutions of this model with those of the transport equation for electrons in suspended monolayer graphene. A numerical scheme based on the discontinuous Galerkin method is used for finding the solutions of the electron Boltzmann equation because the same method has been already successfully applied to a more conventional semiconductor material like silicon [9, 10].

Comparison of the physically average quantities, electron energy and velocity, shows that the MEP model is reasonable even if the introduction of some improvements regarding additional moments or nonlinear effects is needed.

2 THE TRANSPORT EQUATIONS FOR ELECTRONS IN GRAPHENE

The electron energy in graphene depends on a two dimensional wave vector \mathbf{k} belonging to a bi-dimensional Brillouin zone which has an hexagonal shape.

The most part of electrons are in the valleys around the vertices of the Brillouin zone, called Dirac points or K and K' points. Usually the K and K' valleys are treated as a single equivalent one.

In a semiclassical kinetic setting, the charge transport in graphene is described by four Boltzmann equations, one for electrons in the valence band (π) and one for electrons in the conduction band (π^*), that in turn can belong to the K or K' valley,

$$\frac{\partial f_{\ell,s}(t, \mathbf{x}, \mathbf{k})}{\partial t} + \mathbf{v}_{\ell,s} \cdot \nabla_{\mathbf{x}} f_{\ell,s}(t, \mathbf{x}, \mathbf{k}) - \frac{e}{\hbar} \mathbf{E} \cdot \nabla_{\mathbf{k}} f_{\ell,s}(t, \mathbf{x}, \mathbf{k}) = \left. \frac{df_{\ell,s}}{dt}(t, \mathbf{x}, \mathbf{k}) \right|_{e-ph}, \quad (1)$$

where $f_{\ell,s}(t, \mathbf{x}, \mathbf{k})$ represents the distribution function of charge carriers, band π or π^* ($s = -1$ or $s = 1$), in the valley ℓ (K or K'), at position \mathbf{x} , time t and wave-vector \mathbf{k} . We denote by $\nabla_{\mathbf{x}}$ and $\nabla_{\mathbf{k}}$ the gradients with respect to the position and the wave vector, respectively. The microscopic velocity $\mathbf{v}_{\ell,s}$ is related to the band energy $\varepsilon_{\ell,s}$ by

$$\mathbf{v}_{\ell,s} = \frac{1}{\hbar} \nabla_{\mathbf{k}} \varepsilon_{\ell,s}.$$

With a very good approximation [1] a linear dispersion relation holds for the band energies $\varepsilon_{\ell,s}$ around the equivalent Dirac points; so that $\varepsilon_{\ell,s} = s \hbar v_F |\mathbf{k} - \mathbf{k}_{\ell}|$, where v_F is the (constant) Fermi velocity, \hbar the Planck constant divided by 2π , and \mathbf{k}_{ℓ} is the position of the Dirac point ℓ . The elementary (positive) charge is denoted by e , and \mathbf{E} is the electric field obtained by the Poisson equation, which must be coupled with Eq. (1). The right hand side of Eq. (1) is the collision term representing the interaction of electrons with acoustic, optical and K phonons. Acoustic phonon scattering is intra-valley and intra-band. Optical phonon scattering is intra-valley and can be longitudinal optical (LO) and transversal optical (TO); it can be intra-band, leaving the electron in the same band, or

inter-band, pushing the electron from an initial band to another one. Scattering with optical phonon of K type pushes electrons from a valley to a nearby one (inter-valley scattering). We assume that phonons are a bath at thermal equilibrium. Hence, the general form of the collision term can be written as

$$\left. \frac{df_{\ell,s}}{dt}(t, \mathbf{x}, \mathbf{k}) \right|_{e-ph} = \sum_{\ell',s'} \left[\int S_{\ell',s',\ell,s}(\mathbf{k}', \mathbf{k}) f_{\ell',s'}(t, \mathbf{x}, \mathbf{k}') (1 - f_{\ell,s}(t, \mathbf{x}, \mathbf{k})) d\mathbf{k}' - \int S_{\ell,s,\ell',s'}(\mathbf{k}, \mathbf{k}') f_{\ell,s}(t, \mathbf{x}, \mathbf{k}) (1 - f_{\ell',s'}(t, \mathbf{x}, \mathbf{k}')) d\mathbf{k}' \right],$$

where the total collision term is given by the sum of the contributions of the several types of scatterings described above

$$S_{\ell',s',\ell,s}(\mathbf{k}', \mathbf{k}) = \sum_{\nu} \left| G_{\ell',s',\ell,s}^{(\nu)}(\mathbf{k}', \mathbf{k}) \right|^2 \left[(n_{\mathbf{q}}^{(\nu)} + 1) \delta(\varepsilon_{\ell,s}(\mathbf{k}) - \varepsilon_{\ell',s'}(\mathbf{k}') - \hbar\omega_{\mathbf{q}}^{(\nu)}) + n_{\mathbf{q}}^{(\nu)} \delta(\varepsilon_{\ell,s}(\mathbf{k}) - \varepsilon_{\ell',s'}(\mathbf{k}') + \hbar\omega_{\mathbf{q}}^{(\nu)}) \right]. \quad (2)$$

The index ν labels the ν -th phonon mode, $G_{\ell',s',\ell,s}^{(\nu)}(\mathbf{k}', \mathbf{k})$ is the scattering rate, which describes the scattering mechanism, due to the ν -th phonons, between electrons belonging to valley ℓ' and band s' , and electrons belonging to valley ℓ and band s . The symbol δ denotes the Dirac distribution function, $\omega_{\mathbf{q}}^{(\nu)}$ is the ν -th phonon frequency, $n_{\mathbf{q}}^{(\nu)}$ is the Bose-Einstein distribution for the ν -type phonons

$$n_{\mathbf{q}}^{(\nu)} = \frac{1}{e^{\hbar\omega_{\mathbf{q}}^{(\nu)}/k_B T} - 1},$$

where k_B is the Boltzmann constant and T the constant graphene lattice temperature. If, for a phonon ν_* -type, $\hbar\omega_{\mathbf{q}}^{(\nu_*)} \ll k_B T$, then the corresponding scattering can be assumed elastic. In this case, we eliminate in Eq. (2) the term $\hbar\omega_{\mathbf{q}}^{(\nu_*)}$ inside the delta distribution and we use the Laurent approximation $n_{\mathbf{q}}^{(\nu_*)} \approx k_B T / \hbar\omega_{\mathbf{q}}^{(\nu_*)}$.

Electrons which contribute to the charge transport in graphene are those in the conduction and valence band, and it is preferable to treat the latter as holes for insuring the integrability of the corresponding distribution function. Electrons and holes mostly populate the states near to the K and K' valleys. In this paper we consider the case of a high value of the Fermi energy which is equivalent for conventional semiconductors to a n-type doping. Under such a condition electrons belonging to the conduction band do not move to the valence band and vice versa. Therefore the hole dynamics is neglected.

A reference frame centered in the K -point will be used and in order to simplify the notation the indices s and ℓ will be omitted.

Under the above hypotheses the scattering rates read as follows.

For acoustic phonons, we consider the elastic approximation

$$2 n_{\mathbf{q}}^{(ac)} |G^{(ac)}(\mathbf{k}', \mathbf{k})|^2 = \frac{1}{(2\pi)^2} \frac{\pi D_{ac}^2 k_B T}{\hbar \sigma_m v_p^2} (1 + \cos \vartheta_{\mathbf{k}, \mathbf{k}'}), \quad (3)$$

where D_{ac} is the acoustic phonon coupling constant, v_p is the sound speed in graphene, σ_m is the graphene areal density, and $\vartheta_{\mathbf{k},\mathbf{k}'}$ is the convex angle between \mathbf{k} and \mathbf{k}' .

There are three relevant optical phonon scatterings due to the longitudinal optical (LO), the transversal optical (TO) and the K (K) phonons. The related scattering rates are

$$|G^{(LO)}(\mathbf{k}', \mathbf{k})|^2 = \frac{1}{(2\pi)^2} \frac{\pi D_O^2}{2\sigma_m \omega_O} (1 - \cos(\vartheta_{\mathbf{k},\mathbf{k}'-\mathbf{k}} + \vartheta_{\mathbf{k}',\mathbf{k}'-\mathbf{k}})) \quad (4)$$

$$|G^{(TO)}(\mathbf{k}', \mathbf{k})|^2 = \frac{1}{(2\pi)^2} \frac{\pi D_O^2}{2\sigma_m \omega_O} (1 + \cos(\vartheta_{\mathbf{k},\mathbf{k}'-\mathbf{k}} + \vartheta_{\mathbf{k}',\mathbf{k}'-\mathbf{k}})) \quad (5)$$

$$|G^{(K)}(\mathbf{k}', \mathbf{k})|^2 = \frac{1}{(2\pi)^2} \frac{\pi D_K^2}{\sigma_m \omega_K} (1 - \cos \vartheta_{\mathbf{k},\mathbf{k}'}), \quad (6)$$

where D_O is the optical phonon coupling constant, ω_O the optical phonon frequency, D_K is the K-phonon coupling constant and ω_K the K-phonon frequency. The angles $\vartheta_{\mathbf{k},\mathbf{k}'-\mathbf{k}}$ and $\vartheta_{\mathbf{k}',\mathbf{k}'-\mathbf{k}}$ denote the convex angles between \mathbf{k} and $\mathbf{k}' - \mathbf{k}$ and between \mathbf{k}' and $\mathbf{k}' - \mathbf{k}$, respectively.

3 THE NUMERICAL METHOD FOR THE TRANSPORT EQUATION

A numerical approach based on the discontinuous Galerkin method for solving the kinetic model described in Sec. 2 is used.

Since we are interested to the transport properties in a homogeneous suspended monolayer, we look for spatially homogeneous solutions to Eq. (1) with a constant electric field. The Boltzmann equation in the K valley reduces to

$$\begin{aligned} \frac{\partial f(t, \mathbf{k})}{\partial t} - \frac{e}{\hbar} \mathbf{E} \cdot \nabla_{\mathbf{k}} f(t, \mathbf{k}) &= \int S(\mathbf{k}', \mathbf{k}) f(t, \mathbf{k}') (1 - f(t, \mathbf{k})) d\mathbf{k}' \\ &\quad - \int S(\mathbf{k}, \mathbf{k}') f(t, \mathbf{k}) (1 - f(t, \mathbf{k}')) d\mathbf{k}'. \end{aligned} \quad (7)$$

A similar equation holds for the K' valley. As initial condition we take the Fermi-Dirac distribution

$$f(0, \mathbf{k}) = \frac{1}{1 + \exp\left(\frac{\varepsilon(\mathbf{k}) - \varepsilon_F}{k_B T}\right)},$$

where $T = 300 K$, and ε_F is the Fermi energy, which is related to the initial charge density by

$$\rho(0) = \frac{2}{(2\pi)^2} \int f(0, \mathbf{k}) d\mathbf{k}. \quad (8)$$

Eq. (7) is discretized by adopting a discontinuous Galerkin scheme. We choose a bounded domain $\Omega \subset \mathbb{R}^2$ such that $f(t, \mathbf{k}) \approx 0$ for every $\mathbf{k} \notin \Omega$ and $t > 0$, and introduce a finite

decomposition $\{C_\alpha\}_{\alpha=1}^N$ of Ω , with C_α appropriate open sets, such that

$$C_\alpha \cap C_\beta = \emptyset \quad \text{if } \alpha \neq \beta, \quad \text{and} \quad \bigcup_{\alpha=1}^N \overline{C_\alpha} = \Omega.$$

The distribution function is assumed to be constant in each cell C_α . If we denote by $\chi_\alpha(\mathbf{k})$ the characteristic function over the cell C_α , then the approximation of the distribution function f is given by

$$f(t, \mathbf{k}) \approx f^\alpha(t) \quad \forall \mathbf{k} \in C_\alpha \iff f(t, \mathbf{k}) \approx \sum_{\alpha=1}^N f^\alpha(t) \chi_\alpha(\mathbf{k}) \quad \forall \mathbf{k} \in \bigcup_{\alpha=1}^N C_\alpha.$$

This assumption replaces the unknown f , which depends on the two variables t and \mathbf{k} , with a set of N unknowns f^α , which depend only on time t . In order to obtain a set of N equations for the new unknowns f^α , we integrate Eq. (7) with respect to \mathbf{k} over every cell C_α and replace f with its approximation. The derivative of f with respect to the time is treated easily. We have

$$\int_{C_\alpha} \frac{\partial f(t, \mathbf{k})}{\partial t} d\mathbf{k} \approx M_\alpha \frac{d f^\alpha(t)}{dt}$$

where M_α is the measure of the cell C_α . It is clear that the numerical method yields a system of ordinary differential equations by discretizing the collision operator and the drift term as discussed below.

DISCRETIZATION OF THE COLLISION OPERATOR.

Since for each $\mathbf{k} \in C_\alpha$

$$\begin{aligned} & \int S(\mathbf{k}', \mathbf{k}) f(t, \mathbf{k}') (1 - f(t, \mathbf{k})) d\mathbf{k}' - \int S(\mathbf{k}, \mathbf{k}') f(t, \mathbf{k}) (1 - f(t, \mathbf{k}')) d\mathbf{k}' \\ & \approx \sum_{\beta=1}^N \left[\int_{C_\beta} S(\mathbf{k}', \mathbf{k}) f^\beta(t) (1 - f^\alpha(t)) d\mathbf{k}' - \int_{C_\beta} S(\mathbf{k}, \mathbf{k}') f^\alpha(t) (1 - f^\beta(t)) d\mathbf{k}' \right] \\ & = \sum_{\beta=1}^N \left[f^\beta(t) (1 - f^\alpha(t)) \int_{C_\beta} S(\mathbf{k}', \mathbf{k}) d\mathbf{k}' - f^\alpha(t) (1 - f^\beta(t)) \int_{C_\beta} S(\mathbf{k}, \mathbf{k}') d\mathbf{k}' \right], \end{aligned}$$

if we define

$$A^{\alpha, \beta} = \int_{C_\alpha} \left[\int_{C_\beta} S(\mathbf{k}, \mathbf{k}') d\mathbf{k}' \right] d\mathbf{k}, \quad (9)$$

then we obtain

$$\begin{aligned} & \int_{C_\alpha} \left[\int S(\mathbf{k}', \mathbf{k}) f(t, \mathbf{k}') (1 - f(t, \mathbf{k})) d\mathbf{k}' - \int S(\mathbf{k}, \mathbf{k}') f(t, \mathbf{k}) (1 - f(t, \mathbf{k}')) d\mathbf{k}' \right] d\mathbf{k} \\ & \approx \sum_{\beta=1}^N [A^{\beta, \alpha} (1 - f^\alpha(t)) f^\beta(t) - A^{\alpha, \beta} f^\alpha(t) (1 - f^\beta(t))]. \end{aligned}$$

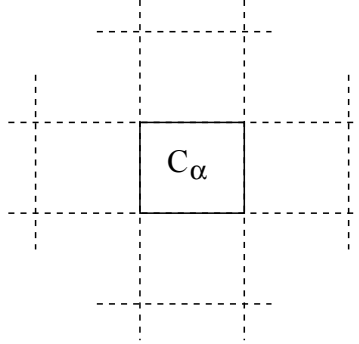


Figure 1: Cells employed for the numerical flux in the case of a simple rectangular grid.

So doing, the integral collision operator is replaced by quadratic polynomials. We note that the numerical coefficients $A^{\alpha,\beta}$ depend only on the scattering terms and the domain decomposition.

DISCRETIZATION OF THE FORCE TERM.

We must approximate the term

$$-\frac{e}{\hbar} \mathbf{E} \cdot \int_{C_\alpha} \nabla_{\mathbf{k}} f(t, \mathbf{k}) d\mathbf{k} = -\frac{e}{\hbar} \mathbf{E} \cdot \int_{\partial C_\alpha} f(t, \mathbf{k}) \mathbf{n} d\sigma$$

where \mathbf{n} is the external unit normal to the boundary ∂C_α of the cell C_α . Since, due to the Galerkin method, the approximation of f is not defined on the boundary of the cells, we must introduce a *numerical flux*, that furnishes reasonable values of f on every ∂C_α , depending on the values of the approximation of f in the nearest neighborhood of the cell C_α and on the sign of $\mathbf{E} \cdot \mathbf{n}$. In Fig. 1 we show a simple picture of the cells that can be involved to find the numerical flux. The simplest numerical flux is given by the *upwind rule*, that uses only the four nearest adjacent cells.

4 CARRIER MOMENT EQUATIONS AND CLOSURE RELATIONS

Macroscopic quantities can be defined as moments of the distribution functions with respect to some suitable weight functions $\psi(\mathbf{k})$, assuming a sufficient regularity for the existence of the involved integrals. In particular for electrons and holes, we propose a set of moment equations consisting of the balance equations of the following quantities

$$\begin{aligned}
\text{average density} \quad \rho_i &= \frac{4}{(2\pi)^2} \int_{\mathbb{R}^2} f_i(t, \mathbf{x}, \mathbf{k}) d\mathbf{k}, \\
\text{average velocity} \quad \rho_i \mathbf{V}_i &= \frac{4}{(2\pi)^2} \int_{\mathbb{R}^2} f_i(t, \mathbf{x}, \mathbf{k}) \mathbf{v} d\mathbf{k}, \\
\text{average energy} \quad \rho_i W_i &= \frac{4}{(2\pi)^2} \int_{\mathbb{R}^2} f_i(t, \mathbf{x}, \mathbf{k}) \varepsilon d\mathbf{k}, \\
\text{average energy-flux} \quad \rho_i \mathbf{S}_i &= \frac{4}{(2\pi)^2} \int_{\mathbb{R}^2} f_i(t, \mathbf{x}, \mathbf{k}) \varepsilon \mathbf{v} d\mathbf{k},
\end{aligned}$$

($i = \text{electron, hole}$), where the factor 4 arises from taking into account both the spin states and the two equivalent valleys.

By integrating the Boltzmann equations with respect to \mathbf{k} , one has the following balance equations for the above-defined macroscopic quantities

$$\frac{\partial}{\partial t} \rho_i + \nabla_{\mathbf{r}} \cdot (\rho_i \mathbf{V}_i) = \rho_i C_i, \quad (10)$$

$$\frac{\partial}{\partial t} (\rho_i \mathbf{V}_i) + \nabla_{\mathbf{r}} \cdot (\rho_i \mathbf{F}_i^{(0)}) + \mathbf{e}_i \rho_i \mathbf{G}_i^{(0)} \mathbf{E} = \rho_i C_{\mathbf{V}_i}, \quad (11)$$

$$\frac{\partial}{\partial t} (\rho_i W_i) + \nabla_{\mathbf{r}} \cdot (\rho_i \mathbf{S}_i) + \mathbf{e}_i \rho_i \mathbf{E} \cdot \mathbf{V}_i = \rho_i C_{W_i}, \quad (12)$$

$$\frac{\partial}{\partial t} (\rho_i \mathbf{S}_i) + \nabla_{\mathbf{r}} \cdot (\rho_i \mathbf{F}_i^{(1)}) + \mathbf{e}_i \rho_i \mathbf{G}_i^{(1)} \mathbf{E} = \rho_i C_{\mathbf{S}_i}, \quad (13)$$

where the G 's and F 's are extra-fluxes and the terms at the right hand sides are productions (the reader is referred to [7] for details) and \mathbf{e}_i is equal to e for electrons and $-e$ for holes.

The extra fluxes and the production terms are additional unknown quantities. For them constitutive relations in terms of the fundamental variables are needed in order to get a closed system of balance equations. A well theoretically founded way to get the desired closure relations is to resort to the Maximum Entropy Principle (MEP) [11], according to which the electron and hole distribution functions can be estimated by the distributions $f_{e,MEP}$ and $f_{h,MEP}$ solving the following problem

$$(f_{e,MEP}, f_{h,MEP}) = \max_{f_e(t, \mathbf{x}), f_h(t, \mathbf{x}) \in \mathcal{F}(\mathbb{R}^2)} S[f_e, f_h],$$

under the constraints

$$\begin{aligned}
\begin{pmatrix} \rho_i \\ \rho_i W_i \end{pmatrix} &= \frac{4}{(2\pi)^2} \int_{\mathbb{R}^2} \begin{pmatrix} 1 \\ \varepsilon \end{pmatrix} f_i(t, \mathbf{x}, \mathbf{k}) d\mathbf{k}, \\
\begin{pmatrix} \rho_i \mathbf{V}_i \\ \rho_i \mathbf{S}_i \end{pmatrix} &= \frac{4}{(2\pi)^2} \int_{\mathbb{R}^2} f_i(t, \mathbf{x}, \mathbf{k}) \begin{pmatrix} \mathbf{v} \\ \varepsilon \mathbf{v} \end{pmatrix} d\mathbf{k},
\end{aligned}$$

where $S[f_e, f_h]$ is the total entropy of the system (remind that the phonons are assumed to represent a thermal bath kept at constant temperature and therefore they add a constant contribution to the entropy) given by

$$-k_B \left\{ \frac{4}{(2\pi)^2} \int_{\mathbb{R}^2} [f^e \ln f^e + (1 - f^e) \ln (1 - f^e)] d\mathbf{k} + \frac{4}{(2\pi)^2} \int_{\mathbb{R}^2} [f^h \ln f^h + (1 - f^h) \ln (1 - f^h)] d\mathbf{k} \right\},$$

$\mathcal{F}(\mathbb{R}^2)$ being the space of the distribution functions that admit the moments required as constraints.

By solving the above maximization problem we get

$$f_i = \frac{1}{1 + \exp(\lambda_i + \lambda_{W_i} \varepsilon + \mathbf{v} \cdot (\lambda \mathbf{v}_i + \varepsilon \lambda \mathbf{s}_i))}.$$

As in [12] we linearize the distributions around their isotropic part, obtaining

$$f_i \approx \frac{1}{e^{\lambda_i + \lambda_{W_i} \varepsilon} + 1} \left[1 - \frac{e^{\lambda_i + \lambda_{W_i} \varepsilon}}{e^{\lambda_i + \lambda_{W_i} \varepsilon} - 1} \mathbf{v} \cdot (\lambda \mathbf{v}_i + \varepsilon \lambda \mathbf{s}_i) \right],$$

where the λ 's are Lagrange multipliers which have to be expressed as functions of the state variables by taking into account the constraints.

After that, these distributions are inserted into the kinetic definitions of the additional variables, so closing the system of the balance equations (see [7] for the details).

5 NUMERICAL SOLUTIONS

We want to assess the validity of the MEP hydrodynamical model by a comparison with the solutions furnished by the direct integration of the transport equation. For solving the latter let us consider a circle as domain Ω . A TVD third order Runge-Kutta scheme is used to solve the resulting ODE system similarly to Ref. [13]. We remark that the numerical scheme guarantees the mass conservation.

The Fermi level is set equal to 0.4 eV, a value high enough for neglecting the inter-band interactions, and the lattice constant is kept equal to 300 K. In the literature there are several values for the coupling constants entering into the collision terms. For example for the acoustic deformation potential one can find values ranging from 2.6 eV to 29 eV. Similar degree of uncertainty is found for the optical and K phonon coupling constants as well.

We have performed numerical simulations of a suspended monolayer graphene by considering the parameters used in [14]. The solutions do not depend on \mathbf{x} and therefore we neglect the terms in divergence form in the balance equations (10)-(13), that become a

system of ODEs. Moreover only the component of the velocity and the energy-flux along the direction of the electric field, which we assume to be the x axis, is changing with time if we set the initial velocity equal to zero. Regarding the initial conditions of the other macroscopic variables, consistently with an initial Fermi-Dirac distribution for Eq. (7), we assume zero energy-flux while the initial density and the average energy density are calculated from the initial Fermi-Dirac distribution.

Eq. (7) and the system (10)-(13) have been solved for different values of the applied electric field and the results for the average velocity and the energy are shown in Figs 2, 3.

Regarding the average energy the results of the MEP model are quite satisfactory. In the steady regime the maximum relative error is about 5 % and is reached when $E = 10$ kV/cm. In the other case we have a relative error of 1.4 % for $E = 2$ kV/cm, 2.4 % for $E = 4$ kV/cm, 3 % for $E = 20$ kV/cm. Note that the error is not monotone with respect to the electric field.

The behavior of the relative error for the velocity is different. This latter, instead, is decreasing by increasing the applied field. The discrepancy has a maximum for $E = 2$ kV/cm of about 32 %. For $E = 4$ kV/cm the relative error is 28 %, for $E = 10$ kV/cm 19 %, for $E = 20$ kV/cm 4 %.

In order to understand if the Fermi energy influences the accuracy of the MEP model, we have performed the same simulations with $\varepsilon_F = 0.6$ eV. The qualitative behaviour is similar to the case $\varepsilon_F = 0.4$ eV. Again one finds a relative error for the energy not greater than 5 %. Instead the relative error of the velocity is higher: 37 % if $E = 2$ kV/cm, 32 % if $E = 4$ kV/cm, 30 % $E = 10$ kV/cm, 24 % $E = 20$ kV/cm.

Although the overall discrepancy is reasonable for the applications, it is likely that one needs to include some nonlinear terms in the velocity and the energy-flux or additional moments. Apparently the MEP model under consideration is not able to give a correct equilibrium limit. This is an open problem we are working on.

Acknowledgements

The authors acknowledge the financial support by the project FIR 2014, University of Catania.

REFERENCES

- [1] Castro Neto, A.H., Guinea, F., Peres, N.M.R., Novoselov, K.S., Geim, A.K. The electronic properties of graphene. *Rev. of Mod. Phys.* (2009) **81**:109-162.
- [2] Shishir, R. S. and Ferry, D.K. Velocity saturation in intrinsic graphene. *J. Phys. Condens. Matter* (2009) **21**:344201 .
- [3] Fang, T., Konar, A., Xing, H. and Jena, D. High-field transport in two-dimensional graphene. *Phys. Rev. B* (2011) **84**:125450.

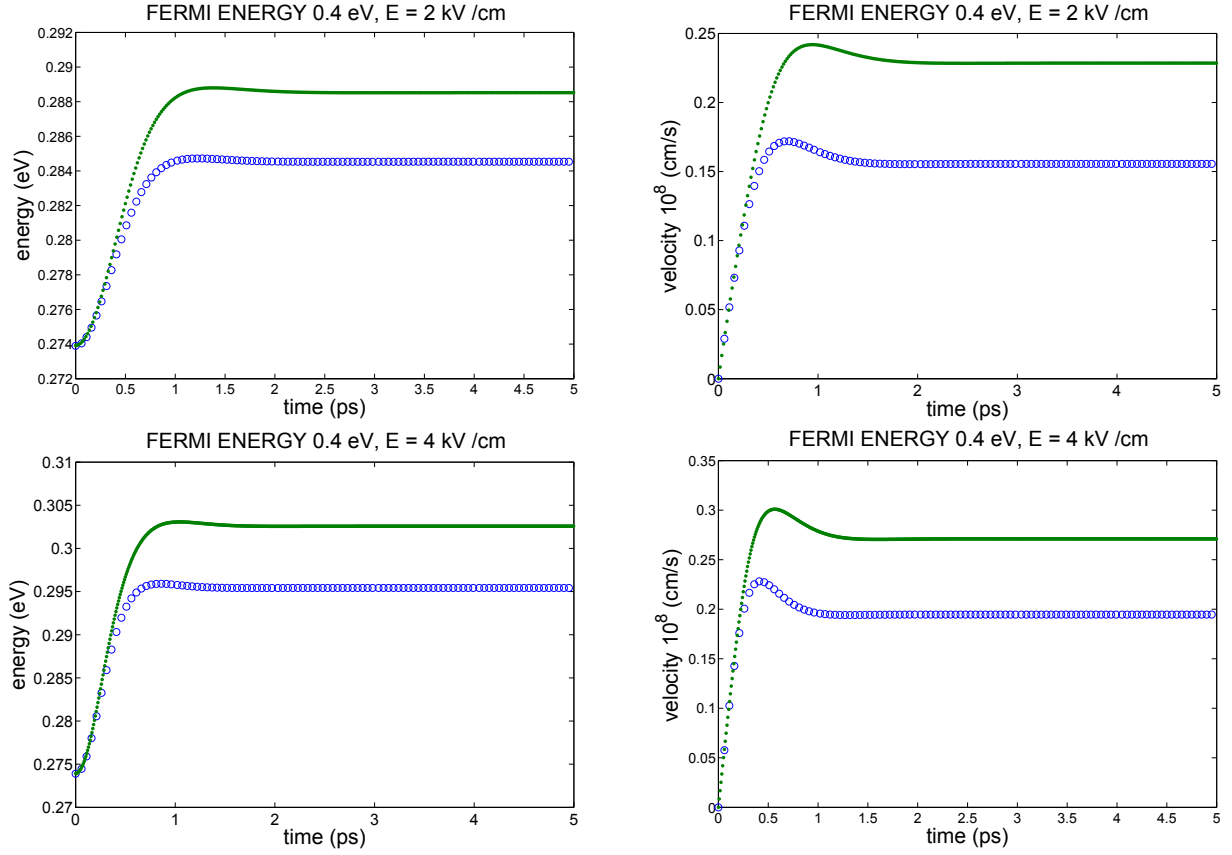


Figure 2: Comparison of the energy and the velocity obtained with a direct solution of the Boltzmann equation (points) and the MEP hydrodynamical model (circles) for the electric fields $E = 2$ kV/cm, $E = 4$ kV/cm by using the same values of the scattering parameters as in [14], by considering a constant lattice temperature of 300 K and a Fermi energy equal to 0.4 eV.

- [4] Tomadin, A., Brida, D., Cerullo, G., Ferrari, A.C. and Polini, M. Nonequilibrium dynamics of photoexcited electrons in graphene: Collinear scattering, Auger processes, and the impact of screening. *Phys. Rev. B* (2013) **88**:035430.
- [5] Lichtenberger, P., Morandi, O. and Schürerer, F. High-field transport and optical phonon scattering in graphene. *Physical Review B* (2011) **84**:045406.
- [6] Zamponi, N. and Barletti, L. Quantum electronic transport in graphene: a kinetic and fluid-dynamical approach. *Math. Methods Appl. Sci.* (2011) **34**:807-818 .
- [7] Camiola, V.D. and Romano, V. Hydrodynamical model for charge transport in graphene. *Journal of Statistical Physics* (2014) **157**:11141137.

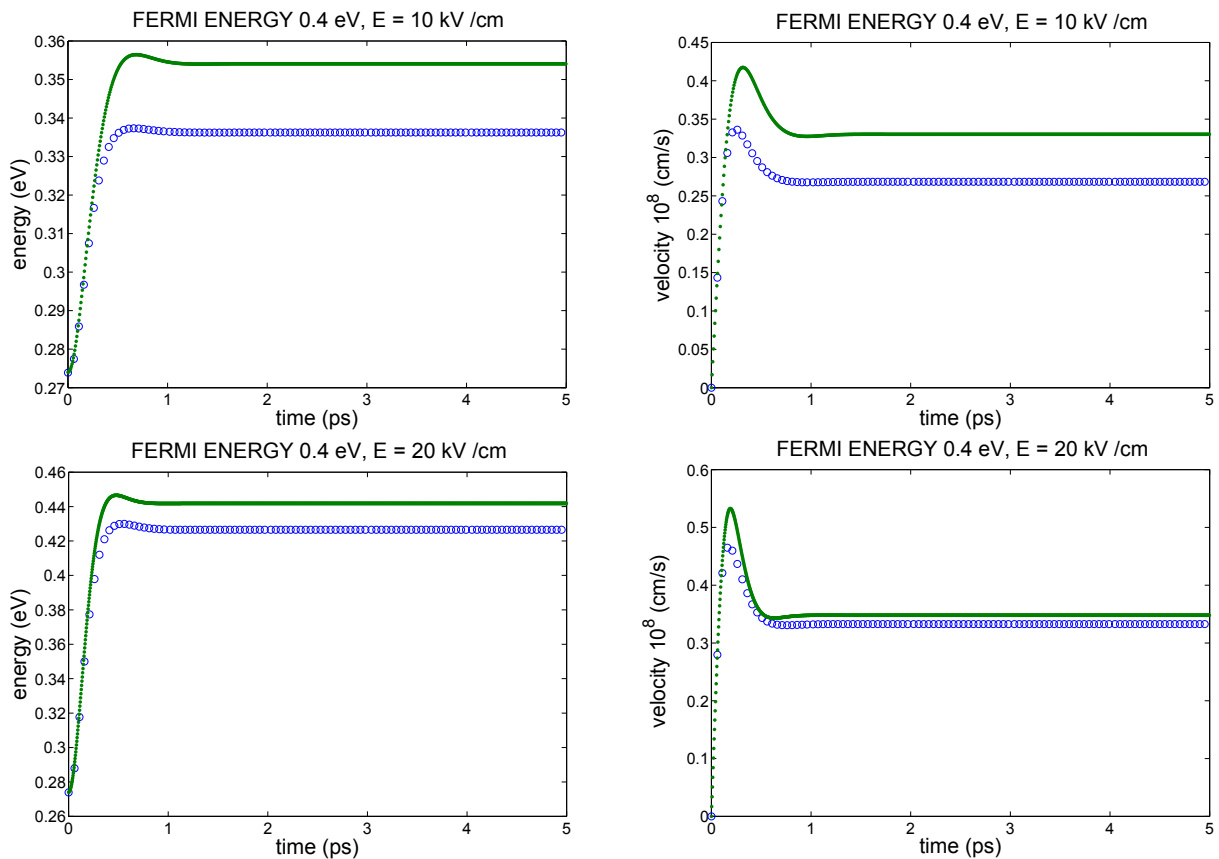


Figure 3: Comparison of the energy and the velocity obtained with a direct solution of the Boltzmann equation (points) and the MEP hydrodynamical model (circles) for the electric fields $E = 10$ kV/cm, $E = 20$ kV/cm by using the same values of the scattering parameters as in [14], by considering a constant lattice temperature of 300 K and a Fermi energy equal to 0.4 eV.

- [8] Mascali, G. and Romano, V. A comprehensive hydrodynamical model for charge transport in graphene. 978-1-4799-5433-9/14/\$31.00 © 2014 IEEE, IWCE-2014 Paris (2014).
- [9] Cheng, Y., Gamba, I.M., Majorana, A., Shu, C.W. A discontinuous Galerkin solver for Boltzmann-Poisson systems in nano devices. *Computer Methods in Applied Mechanics and Engineering* (2009) **198** (37-40):3130–3150.
- [10] Cheng, Y., Gamba, I.M., Majorana, A., Shu, C.W. A brief survey of the discontinuous Galerkin method for the Boltzmann-Poisson equations. *Boletín de la Sociedad Española de Matemática Aplicada* (2011) **54**:47-64 .
- [11] Jaynes, E.T. Information Theory and Statistical Mechanics. *Phys. Rev. B* (1957) **106**:620-630.

- [12] Camiola, V.D., Mascali, G., Romano, V. Simulation of a Double-Gate MOSFET by a Nonparabolic Hydrodynamical Subband Model for Semiconductors Based on the Maximum Entropy Principle. *Mathematical and Computer Modelling* (2013) **58**:321-343.
- [13] Galler, M. and Majorana, A. Deterministic and Stochastic Simulations of Electron Transport in Semiconductors. *Bulletin of the Institute of Mathematics - Academia Sinica - New Series* (2007) **2**:349-365.
- [14] Borysenko, K.M., Mullen, J.T., Barry, E.A., Paul, S., Semenov, Y.G., Zavada, J.M., Buongiorno Nardelli, M. and Kim, K.W. First-principles analysis of electron-phonon interactions in graphene. *Phys. Rev. B* (2010) **11**:121412(R).